CRYSTAL GROWTH & DESIGN

pubs.acs.org/crystal

Article

Solvent Effect on the Preparation of Ionic Cocrystals of DL-Amino Acids with Lithium Chloride: Conglomerate versus Racemate Formation

Published as part of a Crystal Growth and Design virtual special issue in Celebration of the Career of Roger Davey

Oleksii Shemchuk, Enrico Spoletti, Dario Braga, and Fabrizia Grepioni*

Cite This: *Cryst. Growth Des.* 2021, 21, 3438−3448

Read Online

ACCESS | Metrics & More | Article Recommendations | Supporting Information

ABSTRACT: The hydrophobic DL-amino acids alanine, valine, leucine, and isoleucine have been cocrystallized with LiCl via solid-state and solution methods, and the effect of preparation conditions and solvent choice on the racemic versus conglomerate formation has been investigated. For the sake of comparison, enantiopure L-amino acids have also been reacted with LiCl in the same experimental conditions. With DL-alanine only, a racemic ionic cocrystal of formula DL-alanine·LiCl·H_2O is obtained, irrespective of the preparation conditions, while the amino acids DL-valine and DL-leucine undergo spontaneous chiral resolution when MeOH is used in ball milling conditions, yielding monohydrated conglomerates, which at ambient conditions convert over time into the racemic ionic cocrystals DL-Val·LiCl·H_2O and DL-Leu·LiCl·1.5H_2O; these racemic ionic cocrystals (ICCs) are otherwise obtained in a single step if water is employed instead of MeOH, both in ball milling and solution conditions. DL-Isoleucine behaves differently, and product characterization is complicated by the presence of DL-alloisoleucine (DL-aIle) in the commercial starting material; solution crystallization in the presence of excess LiCl, however, unexpectedly results in the formation of the alloisoleucine conglomerate D-aIle·LiCl·H_2O and L-aIle·LiCl·H_2O, together with unreacted DL-isoleucine. Solid-state syntheses of the ionic cocrystals proceed in most cases via formation of intermediate metastable polymorphs; phase identification and structural characterization for all ICCs have been conducted via single crystal and/or powder X-ray diffraction.

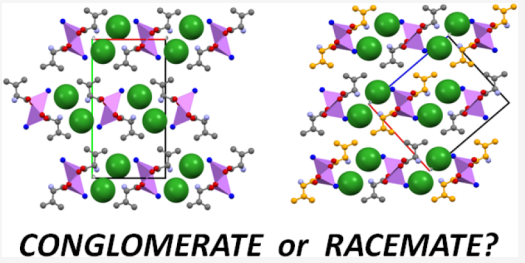

INTRODUCTION

Cocrystallization has developed into an extremely attractive approach toward the formulation of new materials with active principles, providing a means to tune their physicochemical properties in their solid state. As a result, cocrystals, both molecular and ionic, find applications, among others, in the fields of pharmaceuticals,[1−4] agrochemicals,[5−7] high-energy materials,[8−10] and nutraceuticals.[11−13] Ionic cocrystals (ICCs) constitute a class of multicomponent crystalline solids composed of neutral organic molecules and organic or inorganic salts in a defined stoichiometric ratio.[14−20] Pharmaceutical ICCs are of particular interest since the addition of charged components to the active pharmaceutical ingredient (API) of interest *in its crystal* can help in modulating the physicochemical and biological properties of the API (e.g., bioavailability, solubility, intrinsic dissolution rate, morphology, stability toward humidity, thermal stability).[21−24]

A further area where cocrystallization is finding important applications is that of chiral resolution; i.e., cocrystallization can be used for the separation of racemic compounds into their enantiomers. Chiral recognition and enantiomer distinction are fundamental phenomena in chemical and biological systems.[25,26] The formation of molecular[27−36] and ionic[37−39] cocrystals has been demonstrated to be a suitable method to achieve chiral resolution of racemic mixtures. Cocrystallization of the amino acids DL-histidine[37] and DL-proline[38] with lithium halides showed that the Li^+ cations invariably link selectively with amino acids of only one chirality, forming either conglomerates or racemic crystals constituted of homochiral chains, in both anhydrous and hydrated ICCs.[38] It was initially assumed that the tetrahedral geometry around the cation was a prerequisite for the segregation, in individual chains or crystals, of molecules of the same handedness; cocrystallization of the racemic *RS*-etiracetam with $ZnCl_2$, selected because the zinc cation commonly forms tetrahedral complexes,[40] seemed to strengthen this concept; however, $ZnCl_2$ cocrystallization with

Received: February 24, 2021
Revised: April 24, 2021
Published: April 30, 2021

https://doi.org/10.1021/acs.cgd.1c00216
Cryst. Growth Des. 2021, 21, 3438−3448

Scheme 1. Four DL-Amino Acids—in Their Zwitterionic Forms—Reacted with LiCl in the Solid State and in Solution, and the Effect of the Solvent Used on Conglomerate (D-ICC + L-ICC) and Racemic Compounds (DL-ICC) Formation[a]

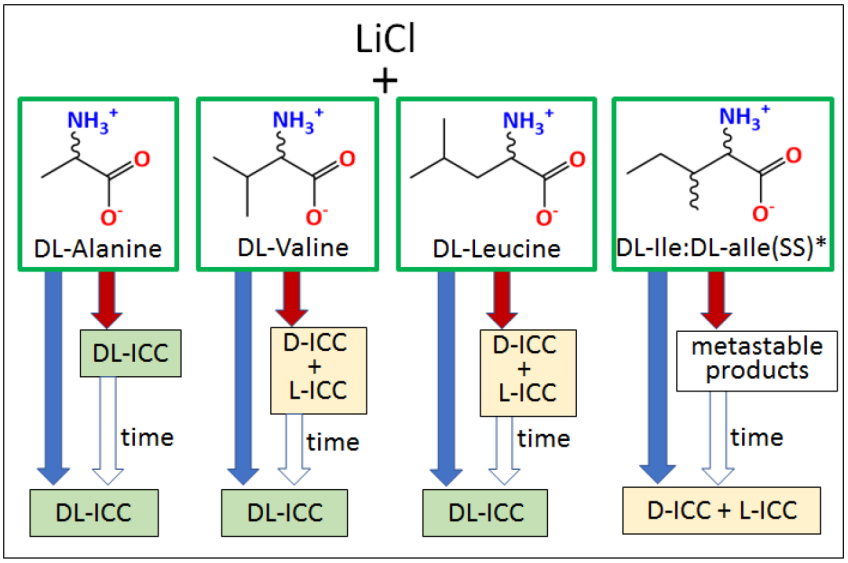

[a]Solvent used: H_2O: blue arrows; MeOH: red arrows. *Commercial DL-isoleucine is a 1:1:1:1 solid solution of L-Ile, D-Ile, L-aIle, and D-aIle.

amino acids showed a less clear-cut preference,[41] as several complexes were formed where the Zn^{2+} cation is coordinated by amino acids of opposite chirality.

We now expand our exploration of the role of lithium chloride, as a coformer in the formation of ionic cocrystals, with a selection of four hydrophobic amino acids both in their enantiopure L- and racemic DL-forms. The cocrystallization experiments were conducted both in the solid state and in solution, and the effect of preparation conditions on conglomerate formation was investigated (see Experimental Section). In the following, besides discussing preparation and characterization of a whole new series of ionic cocrystals of the four amino acids with LiCl, we also report, in the cases of the amino acids DL-valine and DL-leucine, the intriguing observation of a solvent-dependent formation of metastable conglomerates that transform over time into stable racemic end products. We also show that cocrystallization of LiCl with DL-alanine does not lead to chiral resolution, while cocrystallization of LiCl with commercial DL-isoleucine (actually a solid solution of D- and L-isoleucine and of D- and L-alloisoleucine) leads to a complex mixture of conglomerates. Scheme 1 shows a summary of the cocrystallization outcome for the reaction of DL-alanine (DL-Ala), DL-valine (DL-Val), DL-leucine (DL-Leu), and DL-isoleucine (DL-Ile), in their zwitterionic form, with LiCl in the presence of water (blue arrows) or methanol (red arrows). Detailed explanation of all processes and compounds, together with the results of cocrystallization of the enantiopure amino acids with LiCl, are presented in the Results and Discussion.

EXPERIMENTAL SECTION

Materials and Instrumentation. All reagents were purchased from either Merck or TCI Chemicals and used without further purification. It should be noted that the commercial sample of DL-isoleucine also contains the DL-alloisoleucine diastereomeric pair: a single crystal data collection on the starting material yielded the known solid solution structure (vide infra) with an aIle/Ile stoichiometric ratio of 1:1; a Rietveld refinement on the bulk reagent as received was also in agreement with the 1:1 ratio. For all experiments, the highly hygroscopic salt LiCl was dried in the oven at 130 °C for 3 h prior to use.

Solution Synthesis. Single crystals of L-Ala·LiCl·H_2O form II, DL-Ala·LiCl·H_2O form II, L-Val·LiCl·H_2O form II, DL-Val·LiCl·H_2O, and L-Ile·LiCl·H_2O form III were obtained by slow evaporation at RT from undersaturated aqueous solutions (2 mL) of equimolar quantities of the corresponding amino acids and LiCl (0.5 mmol). Single crystals of D-aIle·LiCl·H_2O (conglomerate) were grown at 40 °C from the undersaturated aqueous solutions (5−7 mL) of the corresponding amino acids (0.2 mmol) and a 10-fold excess of LiCl (2.0 mmol). Crystallization from MeOH solutions, tried with all the amino acids discussed here, either yielded the same compounds obtained from water or produced no single crystals.

Solid-State Synthesis. L-Ala·LiCl·H_2O form I, DL-Ala·LiCl·H_2O form I, L-Val·LiCl·H_2O form I, the conglomerate L-Val·LiCl·H_2O + D-Val·LiCl·H_2O form I, L-isoleucine·LiCl·H_2O form I, and the conglomerate D-Leu·LiCl·H_2O + L-Leu·LiCl·H_2O form I were obtained by kneading equimolar quantities of the amino acids and LiCl (0.5 mmol), in the presence of two drops (100 μL) of methanol, for 30 min in a Retsch MM200 ball miller, operated at a frequency of 25 Hz.

L-Ala·LiCl·H_2O form II, DL-Ala·LiCl·H_2O form II, L-Val·LiCl·H_2O form II, DL-Val·LiCl·H_2O, L-Leu·LiCl·H_2O form II, DL-Leu·LiCl·1.5H_2O, L-isoleucine·LiCl·H_2O form III, and the conglomerate L-aIle·LiCl·H_2O + D-aIle·LiCl·H_2O were obtained by kneading the equimolar quantities of the amino acids with LiCl (0.5 mmol), in the presence of one drop (50 μL) of water, for 30 min in a Retsch MM200 ball miller, operated at a frequency of 25 Hz.

In all cases, 10 mL stainless steel vials were used, with one stainless steel ball 7 mm in diameter.

Powder X-ray Diffraction Measurements. Room temperature powder X-ray diffraction (PXRD) patterns were collected on a PANalytical X'Pert Pro automated diffractometer equipped with an X'Celerator detector in Bragg−Brentano geometry, using Cu Kα radiation (λ = 1.5418 Å) without a monochromator in the 2θ range between 3° and 40° (step size: 0.033°; time/step: 20 s; Soller slit: 0,04 rad; antiscatter slit: 1/2; divergence slit: 1/4; 40 mA × 40 kV).

For structure solution purposes, X-ray diffraction patterns were collected on a PANalytical X'Pert Pro automated diffractometer with transmission geometry equipped with a focusing mirror and PIXcel detector, using Cu Kα radiation (λ = 1.5418 Å) without a monochromator in the 2θ range 3−60° (step size 0.0130°, time/step 170.595 s, Soller slit: 0,04 rad; antiscatter slit: 1/2; divergence

https://doi.org/10.1021/acs.cgd.1c00216
Cryst. Growth Des. 2021, 21, 3438−3448

slit: 1/2; 40 kV × 40 mA). To improve the quality of the obtained PXRD patterns, three repetitions were performed, and the scans were merged. Data analyses were carried out using the PANalytical X'Pert Highscore Plus program.

Structural Characterization from Powder Data. Powder diffraction data were analyzed with the software PANalytical X'Pert HighScore Plus. Approximately 15 peaks were chosen in the 2θ range 3−40°, and unit cell parameters were found using the DICVOL4 algorithm. Herein, the structure solution of L-Leu·LiCl·H_2O form I will be described as a case study. A similar approach was applied for all the systems whose structure was solved from PXRD data, namely, L-Val·LiCl·H_2O form I and L-isoleucine·LiCl·H_2O form I and form II. The investigated ICC is characterized by an orthorhombic unit cell with a volume of 1146.61 (1) Å^3—compatible with the presence of an L-leucine molecule, a lithium chloride pair, and one water molecule in the asymmetric unit. The structure was solved in the space group $P2_12_12_1$ by simulated annealing, performed with EXPO2014[42] using the L-leucine molecule in its zwitterionic form and one atom of Li, Cl, and O. Ten runs for simulated annealing trials were set, and a cooling rate (defined as the ratio T_n/T_{n-1}) of 0.95 was used. The best solution was chosen for Rietveld refinement, which was performed with the software TOPAS 5.0.[43] The peak shape was modeled for size and strain with the Gaussian and Lorentzian functions present in TOPAS 5. All the hydrogen atoms were fixed in calculated positions. Refinement converged with χ^2 = 4.38 and R_{wp} = 7.9. Rietveld refinements for all structures solved from powder data are collected in the Supporting Information. Structural data for all compounds investigated in this work are listed in Tables SI-1 to SI-4. It should be noted here that a full structural characterization of the two ICCs L-Leu·LiCl·H_2O form II and DL-Leu·LiCl·1.5H_2O was only obtained by a combination of PXRD and single crystal X-ray diffraction data.

Single Crystal X-ray Diffraction. Single crystal X-ray diffraction data for DL-Ala·LiCl·H_2O form II, L-Ala·LiCl·H_2O form II, DL-Val·LiCl·H_2O form II, L-Val·LiCl·H_2O form II, D-/L-aIle·LiCl·H_2O, L-isoleucine·LiCl·H_2O form III, DL-Leu·LiCl·1.5H_2O, and L-Leu·LiCl·H_2O form II were collected at room temperature with an Oxford Diffraction X'Calibur equipped with a graphite monochromator and a CCD detector. Mo Kα radiation (λ = 0.71073 Å) was used. Unit cell parameters for all compounds discussed herein are reported in Tables SI-1 to SI-4. The structures were solved by the intrinsic phasing methods and refined by least-squares methods against F^2 using SHELXT-2016[44] and SHELXL-2018[45] with the OLEX2 interface.[46] Non-hydrogen atoms were refined anisotropically. Hydrogen atoms were added in calculated positions. The software Mercury 4.0[47] was used for graphic representations. PLATON[48] was used for packing coefficient calculations. Crystal data can be obtained free of charge via www.ccdc.cam.ac.uk/conts/retrieving.html (or from the Cambridge Crystallographic Data Centre, 12 Union Road, Cambridge CB21EZ, UK; fax: (+44) 1223-336-033; or e-mail: deposit@ccdc.cam.ac.uk). CCDC Nos. 2064133−2064144.

RESULTS AND DISCUSSION

In order to investigate the possibility of spontaneous chiral resolution, the racemic amino acids DL-alanine (DL-Ala), DL-valine (DL-Val), DL-leucine (DL-Leu), and DL-isoleucine (DL-Ile), listed in Scheme 1, were cocrystallized with LiCl via liquid assisted grinding (LAG, in ball milling conditions) with MeOH or water, and via solvent evaporation from undersaturated solutions. In parallel, the same methods were applied for the preparation of the corresponding ICCs starting from the enantiopure amino acids L-alanine (L-Ala), L-valine (L-Val), L-leucine (L-Leu), and L-isoleucine (L-Ile), in order to compare the cocrystallization outcomes with those obtained from the racemic ones and identify possible isostructural conglomerates.

A first general observation is that the different preparation methods lead to different cocrystallization outcomes. The racemic versus conglomerate nature of the LAG products in the cases of DL-valine, DL-leucine, and DL-isoleucine appears to depend on whether MeOH or water is used in the ball milling process. Crystallization from water yields different products from those obtained in LAG conditions with MeOH. These last products are, in most cases, metastable forms that convert, with time and in the solid state, toward the more stable phase obtained directly from water. A number of polymorphs is observed; in all cases, the amino acids are in their zwitterionic form, which enables them to bind to the lithium cation via the carboxylate group, while the protonated nitrogen helps in stabilizing the crystal via charge-assisted[49] hydrogen bonding interactions with the chloride anions.

A second general comment may be useful before moving on to describe the individual cases. It will be shown that in all cases discussed in the following intermediate solid phases will be observed. These intermediate crystalline materials (whether resulting from solid-state or solution preparation) will be shown to convert on short or long term into final forms, which no longer change under ambient conditions. These intermediate phases might indeed be thermodynamically *metastable* forms (i.e., polymorphs) or represent different *unstable stoichiometries*. In all cases, the conversion into the final stable forms is brought about by interaction with the atmosphere, i.e., with humidity present. We reckon that while it is useful to know that formation of the end products passes via intermediate transient phases, a detailed knowledge of the role of different quantities of water on the speed of conversion, considering that LiCl is extremely hygroscopic, is beyond the scope of this study.[50−52]

L- and DL-Alanine. The first investigated pair of amino acids was L- and DL-alanine. Initially, the cocrystallization was performed using a mechanochemical approach, i.e., ball milling with MeOH; this process led to the formation of two metastable ICCs (Scheme 2), which, on standing at ambient conditions in an open container, in a matter of a few minutes turned into stable, monohydrated ICCs (see Scheme 1); in the case of L-alanine, the metastable product was always accompanied by a detectable amount of the stable phase

Scheme 2. Cocrystallization of L- and DL-Alanine with LiCl

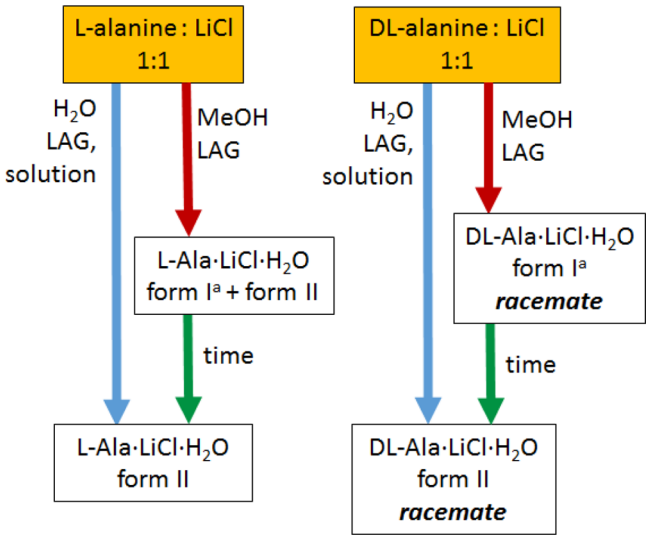

[a]Our hypothesis is that form I, for both L- and DL-ICCs, is a polymorphic modification of the stable form II. Red and blue arrows indicate reactions occurring in the presence of MeOH and water, respectively.

https://doi.org/10.1021/acs.cgd.1c00216
Cryst. Growth Des. 2021, 21, 3438−3448

(see Figure SI-7), even if the ball milling process was stopped after a few minutes. LAG with water or cocrystallization from water led directly to the stable forms. As the transformation occurs in a very short time, our hypothesis is that the final L- and DL-ICCs are polymorphic modifications of the metastable ones: for this reason, they are written as monohydrates form I, while form II is used for the final, stable forms (see Scheme 2).

In L-Ala·LiCl·H_2O form II, the lithium cation is tetrahedrally coordinated by three carboxylate groups of L-alanine and by one water molecule (Figure 1a). Each carboxylate group

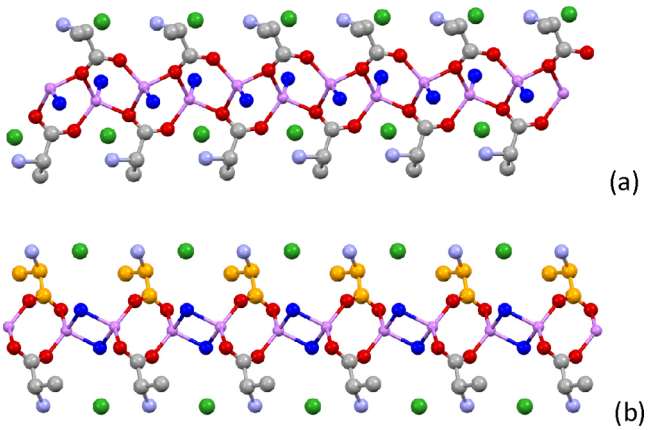

Figure 1. (a) L-Ala·LiCl·H_2O form II: Infinite chains extending along the *a*-axis, with L-alanine zwitterions bridging adjacent lithium cations via the carboxylate groups, and the water molecule directly participating to the tetrahedral coordination (water oxygens in blue). (b) DL-Ala·LiCl·H_2O form II: The chain, extending along the *a*-axis, formed by alanine and water molecules bridging the lithium cations. Different modes of coordination for the alanine and water molecules in L-Ala·LiCl·H_2O form II and DL-Ala·LiCl·H_2O form II can be appreciated. H atoms not shown for clarity.

bridges adjacent lithium cations, resulting in the formation of infinite chains extending along the crystallographic *a*-axis and arranged in layers parallel to the *ac*-plane (Figure 2, left). The chloride ions lie between the layers, at a hydrogen bonding distance to the protonated amino groups and the water molecules.

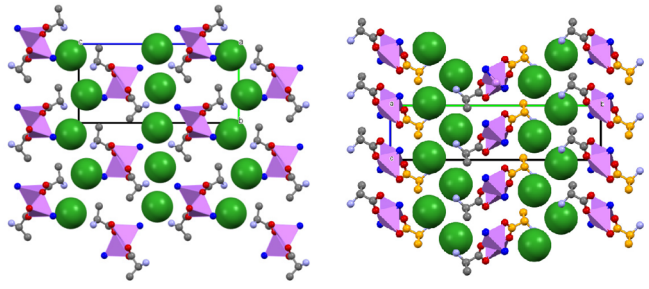

Figure 2. Comparison of the packing patterns in crystalline L-Ala·LiCl·H_2O form II (left) and DL-Ala·LiCl·H_2O form II (right). Views are down the crystallographic *a*-axes. Large green spheres represent the chloride anions. L- and D-Alanine carbon atoms in the DL-Ala·LiCl·H_2O form II are represented by gray and orange spheres. H atoms are not shown for clarity. The tetrahedral coordination around the lithium cations is shown by polyhedral representations.

Tetrahedral coordination around the lithium cations is also observed in DL-Ala·LiCl·H_2O form II; while the water molecules in L-Ala·LiCl·H_2O act as terminal ligands, in the racemic ICC they bridge two adjacent lithium cations, as can be seen in Figure 1b. Each alanine and each water molecule interact with two lithium cations, thus forming an infinite chain extending along the crystallographic *a*-axis; a comparison with the packing of L-Ala·LiCl·H_2O is shown in Figure 2. All attempts to grow single crystals of L-Ala·LiCl·H_2O form I and DL-Ala·LiCl·H_2O form I failed, as the crystallization process invariably yielded the corresponding forms II, regardless of solvent, temperature, or stoichiometric ratio employed.

L- and DL-Valine. The cocrystallization of L- and DL-valine with lithium chloride was initially performed via ball milling with a few drops of methanol. The solid products were analyzed using powder X-ray diffraction. The corresponding diffraction patterns were superimposable (see Figure SI-11), indicating that in the case of DL-valine chiral resolution had taken place upon reaction with LiCl, with formation of conglomerate ICCs (see Scheme 3). Diffraction patterns for

Scheme 3. Cocrystallization of L- and DL-Valine with LiCl

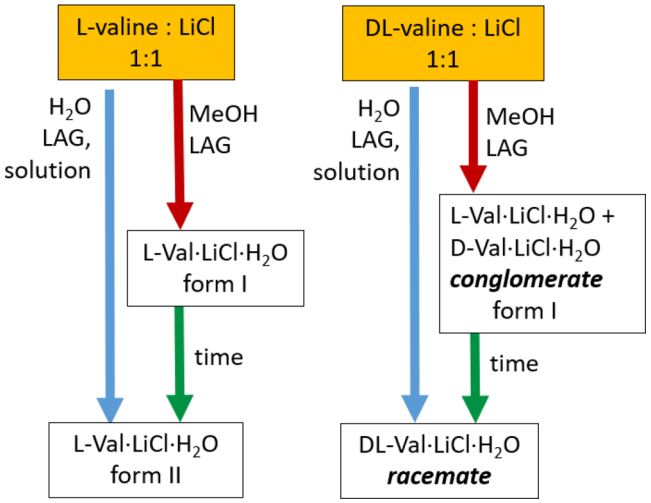

the two crystalline powders were measured again after 24 h: in both cases, a solid state transformation to a second phase had taken place (Figures SI-12 and SI-13).

All attempts to obtain single crystals of L-Val·LiCl·H_2O form I via seeding, crystallization from different solvents, or varying either temperature or stoichiometric ratios employed were unsuccessful. Structural solution from powder data was then attempted; this is usually performed starting from a good data collection in transmission, with the solid sample in a sealed capillary. In the case of L-Val·LiCl·H_2O form I, however, this was not possible, as complete transformation to form II took place in a shorter time with respect to the time necessary for the X-ray data collection. Consequently, the structure of L-Val·LiCl·H_2O form I, which crystallizes in the orthorhombic space group $P2_12_12_1$, was determined from flat-stage data (see Table SI-2).

The ICCs L-Val·LiCl·H_2O form II and racemate DL-Val·LiCl·H_2O, i.e., the final, stable forms obtained upon leaving at ambient conditions for a few minutes the first products of the ball milling with MeOH, were recrystallized from water, and single crystals suitable for X-ray structural characterization could be grown. The two ICCs are quasi-isomorphous[53,54]

https://doi.org/10.1021/acs.cgd.1c00216
Cryst. Growth Des. 2021, 21, 3438−3448

(see Table SI-2); they crystallize in the monoclinic $P2_1$ and $P2_1/n$ space groups, respectively, and are characterized by the presence of infinite chains analogous to those present in L-Ala·LiCl·H_2O form II (see Figure 3 and Figure 4).

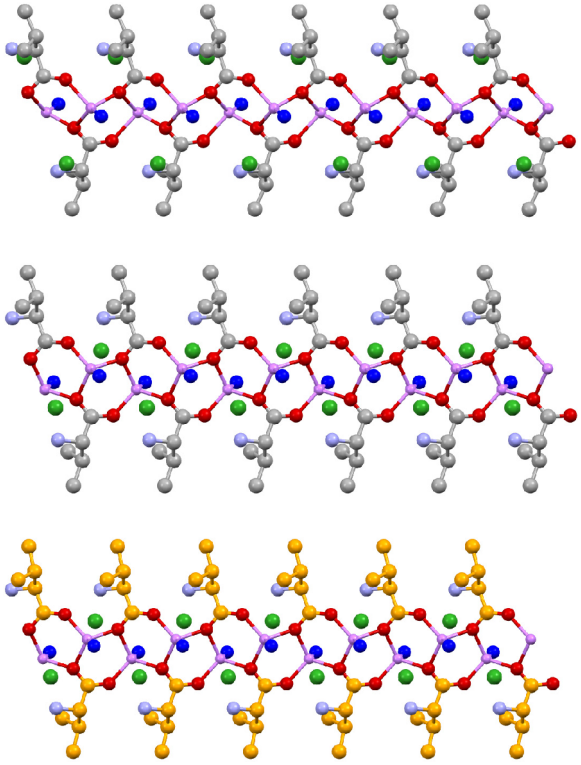

Figure 3. Infinite cationic chains in crystalline L-Val·LiCl·H_2O form I (top, parallel to the *c*-axis direction), L-Val·LiCl·H_2O form II (middle, parallel to the *b*-axis direction), and DL-Val·LiCl·H_2O form II (bottom, parallel to the *b*-axis direction). Note how in the racemate ICC DL-Val·LiCl·H_2O form II the chains are homochiral (only one enantiomer is shown here).

It is worth mentioning that DL-Val·LiCl·H_2O not only forms homochiral chains, but these chains (viewed down the *b*-axis in Figure 3, right) are arranged in "enantiopure layers" parallel to the *bc*-plane. The racemic ICC, therefore, can be seen as a special "cocrystal" of L-Val·LiCl·H_2O and D-Val·LiCl·H_2O (see also Figure 5). This is precisely the chiral preference observed before in the ionic cocrystals of proline and histidine with LiCl.[37]

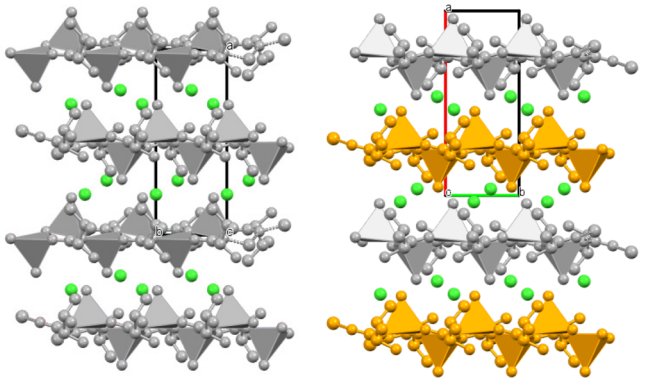

Figure 5. Layers formed by homochiral chains in L-Val·LiCl·H_2O form II (left; cationic chains in gray) and DL-Val·LiCl·H_2O (right; cationic chains containing L-valine in gray and D-valine in orange). Polyhedral representation of the coordination around the lithium cations. H atoms are not shown for clarity.

A comparison between calculated and experimental PXRD patterns (see Figures SI-14 and SI-15) shows that recrystallization from aqueous solutions results in the direct formation of L-Val·LiCl·H_2O form II and DL-Val·LiCl·H_2O form II. This behavior was also observed if the two solids were crystallized from MeOH.

Packing coefficients were estimated for all L-valine ICCs (see Table SI-2); while the value for L-Val·LiCl·H_2O form I, therefore also for the conglomerate, is 0.66, it increases to 0.69 for both L-Val·LiCl·H_2O form II and DL-Val·LiCl·H_2O. This is in keeping with the density rule,[55] which predicts lower coefficients, i.e., less efficient packing, for metastable forms with respect to stable ones.

L- and DL-Leucine. The cocrystallization results of L- and DL-leucine with LiCl are summarized in Scheme 4.

The cocrystallization outcome of L- and DL-leucine with LiCl appears to be similar to the one observed for valine: the PXRD patterns of the ICCs obtained by mechanochemical cocrystallization of enantiopure and racemic leucine with LiCl, in the presence of MeOH, are perfectly superimposable (see Figure SI-16), indicating that the ICC obtained with DL-leucine is a conglomerate. Unfortunately, all the attempts to grow single

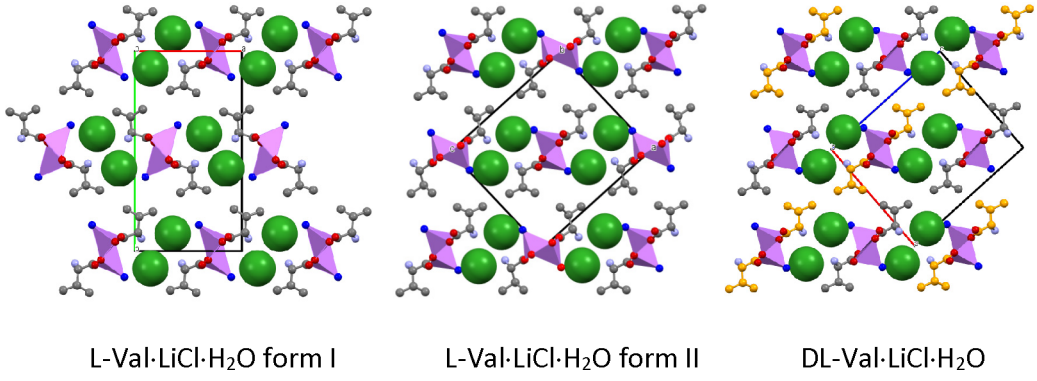

Figure 4. Comparison of crystal packing arrangements in crystalline L-Val·LiCl·H_2O form I (left, view down the *c*-axis), L-Val·LiCl·H_2O form II (middle, view down the *b*-axis), and DL-Val·LiCl·H_2O (right, view down the *b*-axis); note how in the racemic ICC the homochiral chains are organized in layers, parallel to the *bc*-plane (see also Figure 5). H atoms are not shown for clarity.

https://doi.org/10.1021/acs.cgd.1c00216
Cryst. Growth Des. 2021, 21, 3438−3448

Scheme 4. Cocrystallization of L- and DL-Leucine with LiCl

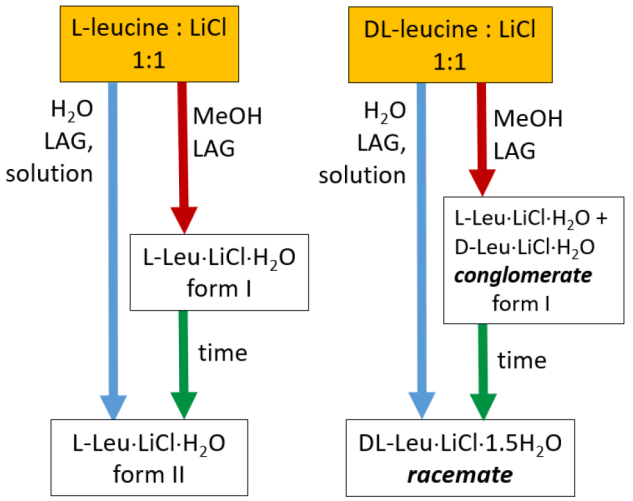

crystals, including evaporation of the solvent at different temperatures, varying the stoichiometric ratios, and seeding with the mechanochemically obtained ICCs (both enantiopure and conglomerate), were unsuccessful. In addition to this, both the enantiopure and the conglomerate ICCs are not stable, and convert to different solid forms if left standing at ambient conditions in open vials for a few minutes. The conversion could be slowed down, however, if the powder was kept in a sealed container. The structure of the L-leucine ICC could thus be solved from powder data, collected on a capillary filled with the polycrystalline powder, which turned out to be L-Leu·LiCl·H_2O form I (see Figure 6).

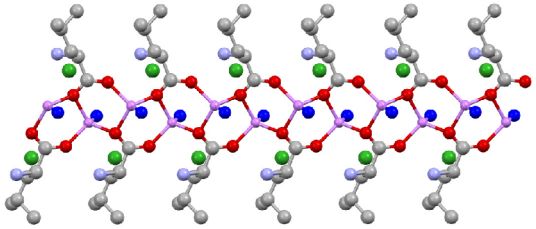

Figure 6. Infinite cationic chains in crystalline L-Leu·LiCl·H_2O form I.

As mentioned above, enantiopure L-Leu·LiCl·H_2O form I and the conglomerate can rapidly convert to stable compounds: this time the patterns of the ICCs obtained from L-leucine and DL-leucine were markedly different from each other (see Figures SI-17 and SI-18).

All attempts to recrystallize these new products invariably led to separation of the reagents, most likely due to their large differences in solubility. Single crystals of moderate quality, however, could be grown as thin needles if an excess of LiCl was employed, and the gross features of the corresponding ICCs, i.e., L-Leu·LiCl·H_2O form II and DL-Leu·LiCl·1.5H_2O, could be obtained. This information was used in turn for structural refinements with good quality powder data on the same compounds (see Table SI-3).

The packing features of the enantiopure L-Leu·LiCl·H_2O form II (see Figure 7) are analogous to those observed for the enantiopure ICCs discussed L-Ala·LiCl·H_2O form II and L-Val·LiCl·H_2O form II discussed above.

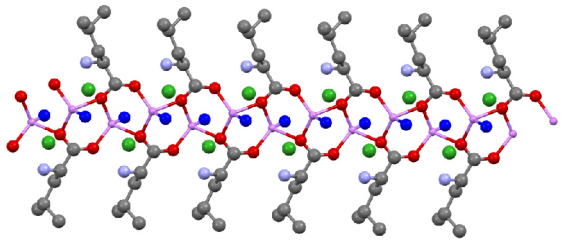

Figure 7. Infinite cationic chains in crystalline L-Leu·LiCl·H_2O Form II. H atoms are not shown for clarity.

The racemic end-product of the process, namely, DL-Leu·LiCl·1.5H_2O, shows a homochiral preference around Li^+ (see Figure 8) as observed in DL-Val·LiCl·H_2O, with formation of

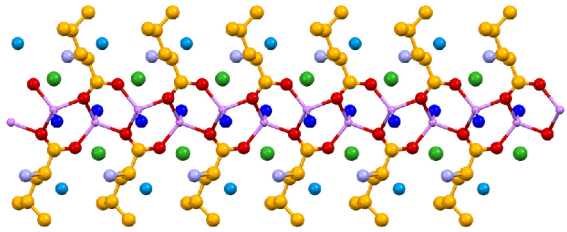

Figure 8. Homochiral chain in DL-Leu·LiCl·1.5H_2O: a screw-axis extending along the chain relates the amino acids on the top side of the chain to those on the bottom side (see also Figure 3, bottom). H atoms are not shown for clarity.

enantiopure layers. In DL-Leu·LiCl·1.5H_2O, however, an additional water, beside the Li^+ coordinated one, acts as a bridge between amino groups and chloride anions in the homochiral chains of $(L\text{-Leu·Li})_n^{n+}/(D\text{-Leu·Li})_n^{n+}$.

A comparison of the crystal packing arrangements of L-Leu·LiCl·H_2O form I, L-Leu·LiCl·H_2O form II, and DL-Leu·LiCl·1.5H_2O is shown in Figure 9. The structural similarity with the arrangements in crystalline L-Val·LiCl·H_2O form I, L-Val·LiCl·H_2O form II, and DL-Val·LiCl·H_2O in Figure 4 is evident.

L-Isoleucine. The cocrystallization of L-isoleucine with LiCl via ball milling with methanol yielded the ICC L-iso·LiCl·H_2O form I, which rapidly transformed into form II (see Scheme 5 and Figure SI-19).

If kept in an open vial, slow decomposition to the starting material was observed. However, if the solid was kept at ambient conditions in a *closed* vial, a slow transformation could be detected to a third form, although the transformation was still not complete after 8 months. This third form, or form III, could be obtained directly when the reaction between L-isoleucine and LiCl was conducted in water solution, or via ball milling in the presence of a drop of water; the solid state transformation of form II into form III could be accelerated in the presence of seeds of form III, obtained via ball milling with water. This behavior confirms the role of MeOH in the nucleation and growth of the intermediate, metastable polymorphs of the ICCs with LiCl.

All attempts to obtain single crystals of L-iso·LiCl·H_2O form I or II were unsuccessful, and their structures had to be determined from powder data. In the case of L-isoleucine·LiCl·H_2O form I, the transformation to form II in capillary was so rapid that flat-stage PXRD data had to be used, while in the case of form II the sample could be placed in a capillary, and transmission geometry could be used for data collection. Both L-isoleucine·LiCl·H_2O form I and form II crystallize in the

https://doi.org/10.1021/acs.cgd.1c00216
Cryst. Growth Des. 2021, 21, 3438−3448

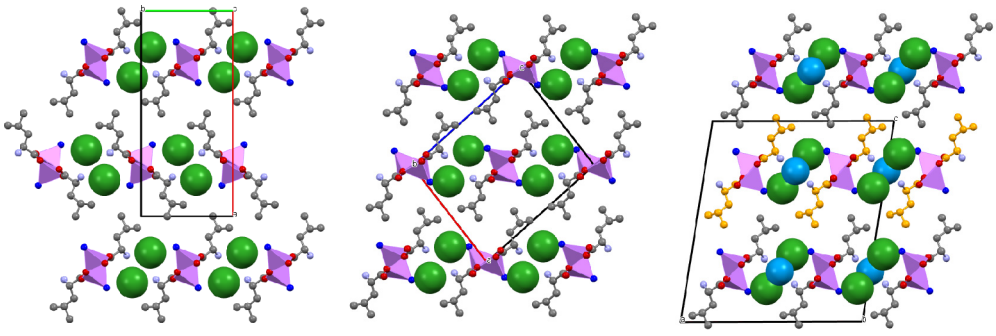

Figure 9. Crystal packing of L-Leu·LiCl·H_2O form I (left), L-Leu·LiCl·H_2O form II (middle), and DL-Leu·LiCl·1.5H_2O (right) (views down the crystallographic *c*-, *b*-, and *b*-axes, respectively). Light-blue spheres represent the water molecules not coordinated to the lithium cations. H atoms are not shown for clarity.

Scheme 5. Cocrystallization of L-Isoleucine with LiCl

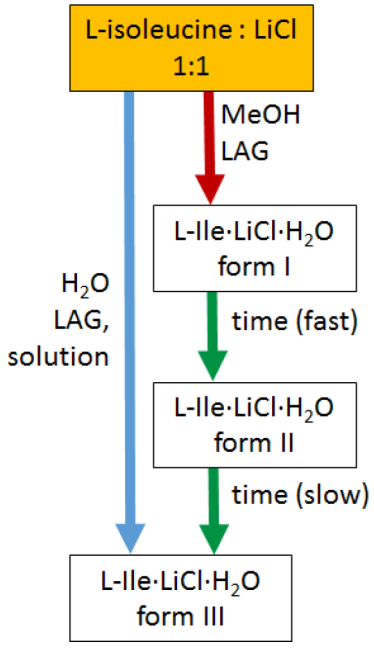

monoclinic system, with extremely similar unit cells (see Table SI-4) and packing features (see Figure 10a,b).

The major difference between all forms is in the conformation of L-isoleucine, as shown in Figure 11.

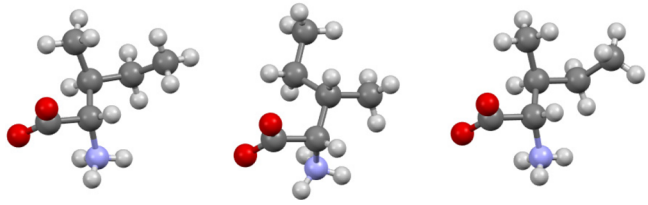

Figure 11. Conformation of L-Ile (in its zwitterionic form) in L-Ile·LiCl·H_2O form I (left), form II (middle), and form III (right).

Single crystals of L-isoleucine·LiCl·H_2O form III could be grown from water solutions; the ICC crystallizes in the orthorhombic system, with a double cell volume with respect to forms I and II. The conformation of L-isoleucine is the same as the one observed for form I (see Figure 11), but the relative arrangement of the cationic chains differs from what was observed either in form I or in form II (see Figure 10). Packing efficiency was estimated via PLATON[48] and found to be lowest in the case of form I (0.65), while the numbers are very similar for forms II and III, being 0.69 and 0.70, respectively (see Table SI-4). This might explain the fast conversion of form I to form II, but both this and the transformation to form III must be mediated by atmospheric water, as form III is the

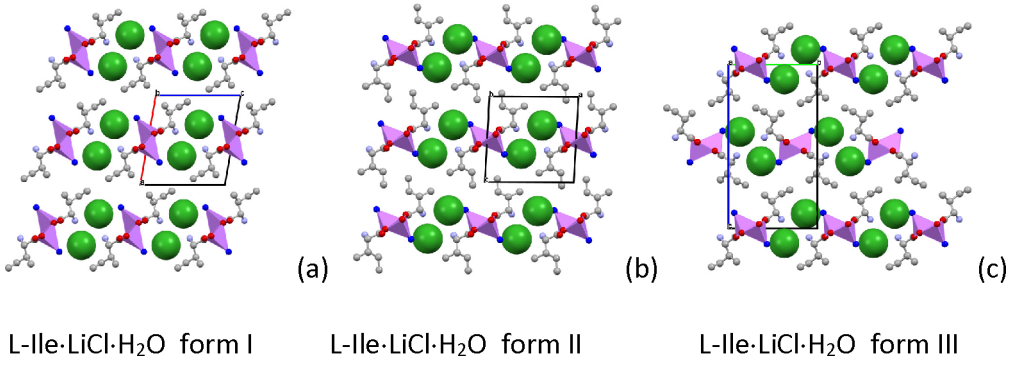

Figure 10. Relative arrangement of the infinite cationic chains in crystalline L-isoleucine·LiCl·H_2O form I (a), form II (b), and form III (c) (views down the crystallographic *b*-, *b*-, and *a*-axes, respectively). H atoms are not shown for clarity.

https://doi.org/10.1021/acs.cgd.1c00216
Cryst. Growth Des. 2021, 21, 3438−3448

only product obtained when water is intentionally used in the reaction with LiCl.

DL-Isoleucine. For the sake of completeness, the formation of ICC of LiCl and DL-isoleucine was also investigated, although the commercially available starting material, as clearly stated by Sigma-Aldrich, is a mixture of the four stereoisomers listed in Scheme 6.

Scheme 6. Four Zwitterionic Stereoisomers Forming the 1:1:1:1 Solid Solution Present in the Commercial Product DL-Isoleucine

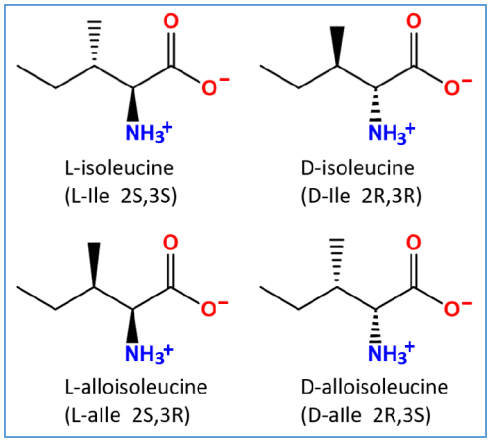

X-ray powder pattern measurements on the commercial form, as well as two single crystal data collections (one crystal taken directly from the commercial sample, a second one recrystallized from water solution), all showed that the four stereoisomers were present in a 1:1:1:1 solid solution, as the pattern is very superimposable to the one for the reported solid solution structure[56] (refcode XADVIH; see Figure SI-21). Hereafter, the term "DL-Ile/DL-aIle(SS)" will be used to indicate such a solid solution.

Not surprisingly, given the presence of four independent chemical entities in the starting material, the behavior of the solid solution upon reaction with LiCl is much more difficult to rationalize with respect to those observed for DL-valine and DL-leucine. Ball milling in the presence of either MeOH or water yields the conglomerate D-aIle·LiCl·H_2O and L-aIle·LiCl·H_2O, together with residual products containing isoleucine (see Figures SI-22 to SI-24). It should be mentioned that also with DL-Ile:DL-aIle(SS) the mechanochemical reaction in the presence of MeOH yields intermediate, metastable compounds (see Figure SI-22), which could not be characterized, with the first one converting rapidly into the second product, which in turn slowly converts to the stable, final product, showing a behavior similar to that of L-isoleucine.

Crystallization of DL-Ile:DL-aIle(SS) and LiCl from an aqueous solution using a 1:1 stoichiometric ratio failed to produce cocrystals, and the reagents precipitated separately. Needle-shaped crystals of the alloisoleucine conglomerate D-aIle·LiCl·H_2O and L-aIle·LiCl·H_2O, however, could be obtained via evaporation at 40 °C of an aqueous solution containing a 10-fold excess of LiCl with respect to DL-isoleucine(SS) (see Scheme 7). In the same crystallization batch affording the alloisoleucine ICC conglomerate, large flat crystals of DL-isoleucine could also be found; as DL-isoleucine and the solid solution isoleucine/alloisoleucine are known to be isomorphous, we cannot exclude the presence of unreacted

Scheme 7. Different Behavior Shown by DL-Ile/DL-aIle(SS)[a] upon Reaction with LiCl in LAG and Solution Conditions[b]

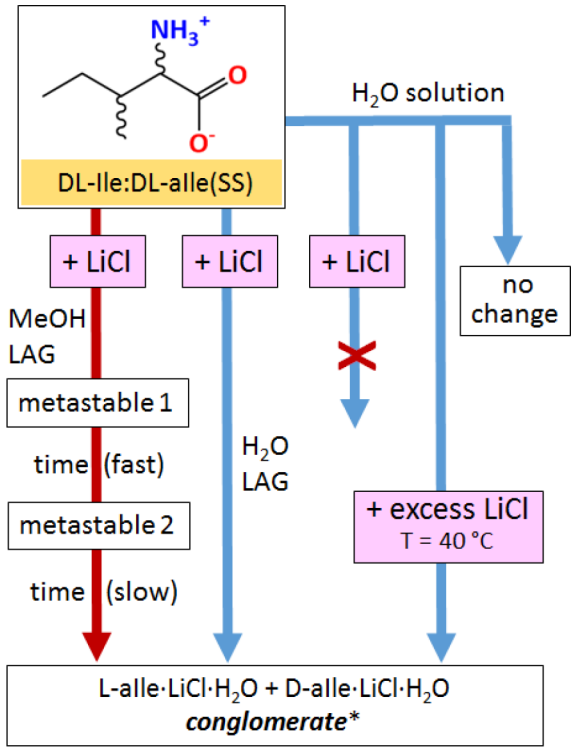

[a]A 1:1:1:1 solid solution of the four stereoisomers in Scheme 6. [b]Recrystallization from water leaves the reagent unchanged. *Isomorphous with L-Ile·LiCl·H_2O form III; DL-isoleucine can be found in all cases together with traces of unidentified material. Single crystals of the stable product are obtained with excess LiCl.

alloisoleucine; still, is interesting to note that only alloisoleucine forms an ionic cocrystal with LiCl, leading to a possible new way to separate the stereoisomers.

The crystal structure of D-aIle·LiCl·H_2O, from the conglomerate, is shown in Figure 12. The alloisoleucine ICC conglomerate is isomorphous with L-Ile·LiCl·H_2O form III (see Table SI-4).

CONCLUSIONS

The cocrystallization of the amino acids alanine, valine, leucine, and isoleucine both as their enantiopure and racemic forms with LiCl resulted in the formation of a series of novel ionic cocrystals. The cocrystallization of both L- and DL-amino acids produced at least two different forms of ICCs (either polymorphs or hydrates). Crystal structures have been determined from either single crystal or powder X-ray diffraction or a combination of.

The idea pursued in this project was not only that of expanding the family of ionic cocrystals of amino acids, a class of compounds that is attracting a growing interest for the potential pharmaceutical implications, but also that of investigating experimental conditions that would favor conglomerate formation, i.e., chiral separation. Cocrystallization with LiCl was chosen as the strategy to follow since it had proven to be efficacious in previous studies.[37,38] In this paper, we have provided further evidence that cocrystallization with LiCl is a suitable technique for spontaneous chiral resolution since the formation of conglomerates was achieved for all the

https://doi.org/10.1021/acs.cgd.1c00216
Cryst. Growth Des. 2021, 21, 3438−3448

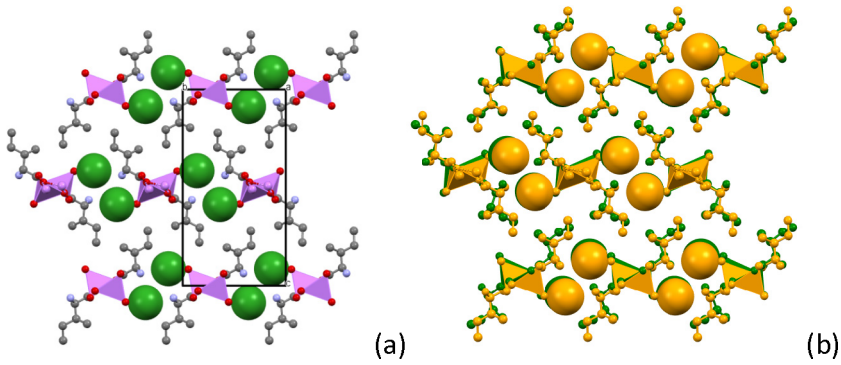

Figure 12. (a) View down the crystallographic *a*-axis of crystalline D-aIle·LiCl·H_2O (from the conglomerate); compare this packing with the one for isomorphous L-Ile ICC form III in Figure 10c. (b) Superimposition of D-aIle ICC (in orange) and L-Ile ICC (in green).

investigated amino acids, with DL-alanine being the only exception. In addition to this, we have also discovered that the solvent used in LAG and/or conventional crystallization also plays an important role in determining the outcome in terms of conglomerate versus racemate formation.

Indeed, the conglomerates with valine and leucine, L-Val·LiCl·H_2O/D-Val·LiCl·H_2O and L-Leu·LiCl·H_2O/D-Leu·LiCl·H_2O, were obtained only via ball milling with methanol, while water led in both cases directly to racemates, DL-Val·LiCl·H_2O and DL-Leu·LiCl·1.5H_2O, respectively. The conglomerates L-Val·LiCl·H_2O/D-Val·LiCl·H_2O and L-Leu·LiCl·H_2O/D-Leu·LiCl·H_2O, however, are unstable toward racemization and convert over time to the same product obtained when water is used directly.

DL-Isoleucine behaved differently, being actually a 1:1:1:1 solid solution of D- and L-isoleucine and D- and L-alloisoleucine. Cocrystallization in warm water solution with an excess of LiCl resulted in the unexpected separation of DL-alloisoleucine from DL-isoleucine, as single crystals of D- and L-aIle·LiCl·H_2O ICCs were recovered, together with single crystals of unreacted DL-isoleucine. Separation of alloisoleucine as an ICC conglomerate was observed also with LAG conditions; in the presence of MeOH, in line with that observed for the previous amino acids, intermediate solids were first obtained which over time transformed in the stable product. Since water is abundant, because of the use of highly hygroscopic LiCl, we tend to favor the hypothesis that the uncharacterized transient forms are polymorphic modifications, and not different solvates, of the final forms. We are planning to further explore the different role of MeOH, and other polar solvents, both in solution and in the solid state, in the chiral processes accompanying ionic cocrystals formation.

■ ASSOCIATED CONTENT

Supporting Information

The Supporting Information is available free of charge at https://pubs.acs.org/doi/10.1021/acs.cgd.1c00216.

Crystallographic details and PXRD patterns are accessible for the structures reported (PDF)

Accession Codes

CCDC 2064133−2064144 contain the supplementary crystallographic data for this paper. These data can be obtained free of charge via www.ccdc.cam.ac.uk/data_request/cif, or by emailing data_request@ccdc.cam.ac.uk, or by contacting The Cambridge Crystallographic Data Centre, 12 Union Road, Cambridge CB2 1EZ, UK; fax: +44 1223 336033.

■ AUTHOR INFORMATION

Corresponding Author

Fabrizia Grepioni − *Molecular Crystal Engineering Laboratory, Dipartimento di Chimica "G. Ciamician", Università di Bologna, 40126 Bologna, Italy;* orcid.org/0000-0003-3895-0979; Email: fabrizia.grepioni@unibo.it

Authors

Oleksii Shemchuk − *Molecular Crystal Engineering Laboratory, Dipartimento di Chimica "G. Ciamician", Università di Bologna, 40126 Bologna, Italy;* orcid.org/0000-0003-3003-3922

Enrico Spoletti − *Molecular Crystal Engineering Laboratory, Dipartimento di Chimica "G. Ciamician", Università di Bologna, 40126 Bologna, Italy*

Dario Braga − *Molecular Crystal Engineering Laboratory, Dipartimento di Chimica "G. Ciamician", Università di Bologna, 40126 Bologna, Italy;* orcid.org/0000-0003-4162-4779

Complete contact information is available at: https://pubs.acs.org/10.1021/acs.cgd.1c00216

Notes

The authors declare no competing financial interest.

■ ACKNOWLEDGMENTS

The University of Bologna (RFO scheme) is acknowledged. We thank Ms. Francesca Suzzi for her help during a high-school science project in our laboratory.

■ REFERENCES

(1) Steed, J. W. The role of co-crystals in pharmaceutical design. *Trends Pharmacol. Sci.* **2013**, *34* (3), 185−93.

(2) Golob, S.; Perry, M.; Lusi, M.; Chierotti, M. R.; Grabnar, I.; Lassiani, L.; Voinovich, D.; Zaworotko, M. J. Improving Biopharmaceutical Properties of Vinpocetine Through Cocrystallization. *J. Pharm. Sci.* **2016**, *105* (12), 3626−3633.

(3) Raheem Thayyil, A.; Juturu, T.; Nayak, S.; Kamath, S. Pharmaceutical Co-Crystallization: Regulatory Aspects, Design, Characterization, and Applications. *Adv. Pharm. Bull.* **2020**, *10* (2), 203−212.

(4) Inam, M.; Liu, L.; Wang, J. W.; Yu, K. X.; Phan, C. U.; Shen, J.; Zhang, W. H.; Tang, G.; Hu, X. Enhancing the Physiochemical Properties of Puerarin via L-Proline Co-Crystallization: Synthesis, Characterization, and Dissolution Studies of Two Phases of Pharmaceutical Co-Crystals. *Int. J. Mol. Sci.* **2021**, *22* (2), 928.

(5) Julien, P. A.; Germann, L. S.; Titi, H. M.; Etter, M.; Dinnebier, R. E.; Sharma, L.; Baltrusaitis, J.; Friscic, T. In situ monitoring of

mechanochemical synthesis of calcium urea phosphate fertilizer cocrystal reveals highly effective water-based autocatalysis. *Chem. Sci.* **2020**, *11* (9), 2350−2355.
(6) Powell, K. A.; Croker, D. M.; Rielly, C. D.; Nagy, Z. K. PAT-based design of agrochemical co-crystallization processes: A case-study for the selective crystallization of 1:1 and 3:2 co-crystals of p-toluenesulfonamide/triphenylphosphine oxide. *Chem. Eng. Sci.* **2016**, *152*, 95−108.
(7) Honer, K.; Kalfaoglu, E.; Pico, C.; McCann, J.; Baltrusaitis, J. Mechanosynthesis of Magnesium and Calcium Salt-Urea Ionic Cocrystal Fertilizer Materials for Improved Nitrogen Management. *ACS Sustainable Chem. Eng.* **2017**, *5* (10), 8546−8550.
(8) Bolton, O.; Simke, L. R.; Pagoria, P. F.; Matzger, A. J. High Power Explosive with Good Sensitivity: A 2:1 Cocrystal of CL-20:HMX. *Cryst. Growth Des.* **2012**, *12* (9), 4311−4314.
(9) Yang, Z.; Li, H.; Zhou, X.; Zhang, C.; Huang, H.; Li, J.; Nie, F. Characterization and Properties of a Novel Energetic-Energetic Cocrystal Explosive Composed of HNIW and BTF. *Cryst. Growth Des.* **2012**, *12* (11), 5155−5158.
(10) Snyder, C. J.; Chavez, D. E.; Imler, G. H.; Byrd, E. F. C.; Leonard, P. W.; Parrish, D. A. Simple and Efficient Synthesis of Explosive Cocrystals containing 3,5-Dimethylpyrazol-1-yl-substituted-1,2,4,5-tetrazines. *Chem. - Eur. J.* **2017**, *23* (65), 16466−16471.
(11) Rosa, J.; Machado, T. C.; da Silva, A. K.; Kuminek, G.; Bortolluzzi, A. J.; Caon, T.; Cardoso, S. G. Isoniazid-Resveratrol Cocrystal: A Novel Alternative for Topical Treatment of Cutaneous Tuberculosis. *Cryst. Growth Des.* **2019**, *19* (9), 5029−5036.
(12) Yadav, B.; Gunnam, A.; Thipparaboina, R.; Nangia, A. K.; Shastri, N. R. Hepatoprotective Cocrystals of Isoniazid: Synthesis, Solid State Characterization, and Hepatotoxicity Studies. *Cryst. Growth Des.* **2019**, *19* (9), 5161−5172.
(13) Xiao, Y.; Zhou, L.; Hao, H.; Bao, Y.; Yin, Q.; Xie, C. Cocrystals of Propylthiouracil and Nutraceuticals toward Sustained-Release: Design, Structure Analysis, and Solid-State Characterization. *Cryst. Growth Des.* **2021**, *21* (2), 1202−1217.
(14) Braga, D.; Grepioni, F.; Maini, L.; Prosperi, S.; Gobetto, R.; Chierotti, M. R. From unexpected reactions to a new family of ionic co-crystals: the case of barbituric acid with alkali bromides and caesium iodide. *Chem. Commun.* **2010**, *46* (41), 7715−7.
(15) Ong, T. T.; Kavuru, P.; Nguyen, T.; Cantwell, R.; Wojtas, L.; Zaworotko, M. J. 2:1 cocrystals of homochiral and achiral amino acid zwitterions with Li+ salts: water-stable zeolitic and diamondoid metal-organic materials. *J. Am. Chem. Soc.* **2011**, *133* (24), 9224−7.
(16) Cheng, H.; Wei, Y.; Wang, S.; Qiao, Q.; Heng, W.; Zhang, L.; Zhang, J.; Gao, Y.; Qian, S. Improving Tabletability of Excipients by Metal-Organic Framework-Based Cocrystallization: a Study of Mannitol and $CaCl_2$. *Pharm. Res.* **2020**, *37* (7), 130.
(17) Meng, X.; Kang, K.; Liu, Y.; Tang, J.; Jiang, X.; Yin, W.; Lin, Z.; Xia, M. Mechanochemical Synthesis of an Ionic Cocrystal with Large Birefringence Resulting from Neutral Planar π-Conjugated Groups. *Cryst. Growth Des.* **2020**, *20* (12), 7588−7592.
(18) Shunnar, A. F.; Dhokale, B.; Karothu, D. P.; Bowskill, D. H.; Sugden, I. J.; Hernandez, H. H.; Naumov, P.; Mohamed, S. Efficient Screening for Ternary Molecular Ionic Cocrystals Using a Complementary Mechanosynthesis and Computational Structure Prediction Approach. *Chem. - Eur. J.* **2020**, *26* (21), 4752−4765.
(19) Marek, P. H.; Cichowicz, G.; Osowicka, D. M.; Madura, I. D.; Dobrzycki, Ł.; Cyrański, M. K.; Ciesielski, A. Polymorphism and structural diversities of LiClO4-β-alanine ionic co-crystals. *CrystEngComm* **2020**, *22* (26), 4427−4437.
(20) Crisan, M.; Petric, M.; Vlase, G.; Vlase, T.; Siminel, A. V.; Bourosh, P. N.; Croitor, L. Organic salt versus salt cocrystal: thermal behavior, structural and photoluminescence investigations. *J. Therm. Anal. Calorim.* **2021**, DOI: 10.1007/s10973-020-10438-y.
(21) Duggirala, N. K.; Smith, A. J.; Wojtas, Ł.; Shytle, R. D.; Zaworotko, M. J. Physical stability enhancement and pharmacokinetics of a lithium ionic cocrystal with glucose. *Cryst. Growth Des.* **2014**, *14* (11), 6135−6142.
(22) Oertling, H. Interactions of alkali-and alkaline earth-halides with carbohydrates in the crystalline state-the overlooked salt and sugar cocrystals. *CrystEngComm* **2016**, *18* (10), 1676−1692.
(23) Song, L.; Robeyns, K.; Tumanov, N.; Wouters, J.; Leyssens, T. Combining API in a dual-drug ternary cocrystal approach. *Chem. Commun.* **2020**, *56* (86), 13229−13232.
(24) Majodina, S.; Ndima, L.; Abosede, O. O.; Hosten, E. C.; Lorentino, C. M. A.; Frota, H. F.; Sangenito, L. S.; Branquinha, M. H.; Santos, A. L. S.; Ogunlaja, A. S. Physical stability enhancement and antimicrobial properties of a sodium ionic cocrystal with theophylline. *CrystEngComm* **2021**, *23* (2), 335−352.
(25) Lammerhofer, M. Chiral recognition by enantioselective liquid chromatography: mechanisms and modern chiral stationary phases. *J. Chromatogr. A* **2010**, *1217* (6), 814−56.
(26) Maier, N. M.; Franco, P.; Lindner, W. Separation of enantiomers: needs, challenges, perspectives. *J. Chromatogr. A* **2001**, *906* (1−2), 3−33.
(27) Springuel, G.; Leyssens, T. Innovative Chiral Resolution Using Enantiospecific Co-Crystallization in Solution. *Cryst. Growth Des.* **2012**, *12* (7), 3374−3378.
(28) Sánchez-Guadarrama, O.; Mendoza-Navarro, F.; Cedillo-Cruz, A.; Jung-Cook, H.; Arenas-García, J. I.; Delgado-Díaz, A.; Herrera-Ruiz, D.; Morales-Rojas, H.; Höpfl, H. Chiral Resolution of RS-Praziquantel via Diastereomeric Co-Crystal Pair Formation with l-Malic Acid. *Cryst. Growth Des.* **2016**, *16* (1), 307−314.
(29) He, L.; Chen, X.; Li, X.; Zhou, Z.; Ren, Z. Chiral co-selector induced chirality switching in the enantioseparation of ofloxacin by forming a co-crystal. *New J. Chem.* **2019**, *43* (38), 15048−15051.
(30) Guillot, M.; de Meester, J.; Huynen, S.; Collard, L.; Robeyns, K.; Riant, O.; Leyssens, T. Cocrystallization-Induced Spontaneous Deracemization: A General Thermodynamic Approach to Deracemization. *Angew. Chem., Int. Ed.* **2020**, *59* (28), 11303−11306.
(31) Li, W.; de Groen, M.; Kramer, H. J. M.; de Gelder, R.; Tinnemans, P.; Meekes, H.; ter Horst, J. H. Screening Approach for Identifying Cocrystal Types and Resolution Opportunities in Complex Chiral Multicomponent Systems. *Cryst. Growth Des.* **2021**, *21* (1), 112−124.
(32) Harfouche, L. C.; Couvrat, N.; Sanselme, M.; Brandel, C.; Cartigny, Y.; Petit, S.; Coquerel, G. Discovery of New Proxyphylline-Based Chiral Cocrystals: Solid State Landscape and Dehydration Mechanism. *Cryst. Growth Des.* **2020**, *20* (6), 3842−3850.
(33) Buol, X.; Caro Garrido, C.; Robeyns, K.; Tumanov, N.; Collard, L.; Wouters, J.; Leyssens, T. Chiral Resolution of Mandelic Acid through Preferential Cocrystallization with Nefiracetam. *Cryst. Growth Des.* **2020**, *20* (12), 7979−7988.
(34) Harfouche, L. C.; Brandel, C.; Cartigny, Y.; Petit, S.; Coquerel, G. Resolution by Preferential Crystallization of Proxyphylline by Using Its Salicylic Acid Monohydrate Co-Crystal. *Chem. Eng. Technol.* **2020**, *43* (6), 1093−1098.
(35) Eddleston, M. D.; Arhangelskis, M.; Friscic, T.; Jones, W. Solid state grinding as a tool to aid enantiomeric resolution by cocrystallisation. *Chem. Commun.* **2012**, *48* (92), 11340−2.
(36) Braga, D.; Grepioni, F.; Lampronti, G. I. Supramolecular metathesis: co-former exchange in co-crystals of pyrazine with (R,R)-, (S,S)-, (R,S)- and (S,S/R,R)-tartaric acid. *CrystEngComm* **2011**, *13* (9), 3122−3124.
(37) Braga, D.; Degli Esposti, L.; Rubini, K.; Shemchuk, O.; Grepioni, F. Ionic Cocrystals of Racemic and Enantiopure Histidine: An Intriguing Case of Homochiral Preference. *Cryst. Growth Des.* **2016**, *16* (12), 7263−7270.
(38) Shemchuk, O.; Tsenkova, B. K.; Braga, D.; Duarte, M. T.; Andre, V.; Grepioni, F. Ionic Co-Crystal Formation as a Path Towards Chiral Resolution in the Solid State. *Chem. - Eur. J.* **2018**, *24* (48), 12564−12573.
(39) Shemchuk, O.; Song, L.; Tumanov, N.; Wouters, J.; Braga, D.; Grepioni, F.; Leyssens, T. Chiral Resolution of RS-Oxiracetam upon Cocrystallization with Pharmaceutically Acceptable Inorganic Salts. *Cryst. Growth Des.* **2020**, *20* (4), 2602−2607.

https://doi.org/10.1021/acs.cgd.1c00216
Cryst. Growth Des. 2021, 21, 3438−3448

(40) Shemchuk, O.; Song, L.; Robeyns, K.; Braga, D.; Grepioni, F.; Leyssens, T. Solid-state chiral resolution mediated by stoichiometry: crystallizing etiracetam with ZnCl2. *Chem. Commun.* **2018**, *54* (77), 10890−10892.
(41) Shemchuk, O.; Grepioni, F.; Braga, D. Co-crystallization of racemic amino acids with ZnCl2: an investigation of chiral selectivity upon coordination to the metal centre. *CrystEngComm* **2020**, *22* (34), 5613−5619.
(42) Altomare, A.; Cuocci, C.; Giacovazzo, C.; Moliterni, A.; Rizzi, R.; Corriero, N.; Falcicchio, A. EXPO2013: a kit of tools for phasing crystal structures from powder data. *J. Appl. Crystallogr.* **2013**, *46* (4), 1231−1235.
(43) Cohelo, A. *TOPAS-Academic*; Coelho Software: Brisbane, Australia, 2007.
(44) Sheldrick, G. M. SHELXT - integrated space-group and crystal-structure determination. *Acta Crystallogr., Sect. A: Found. Adv.* **2015**, *71* (1), 3−8.
(45) Sheldrick, G. M. Crystal structure refinement with SHELXL. *Acta Crystallogr., Sect. C: Struct. Chem.* **2015**, *71* (1), 3−8.
(46) Dolomanov, O. V.; Bourhis, L. J.; Gildea, R. J.; Howard, J. A. K.; Puschmann, H. OLEX2: a complete structure solution, refinement and analysis program. *J. Appl. Crystallogr.* **2009**, *42* (2), 339−341.
(47) Macrae, C. F.; Sovago, I.; Cottrell, S. J.; Galek, P. T. A.; McCabe, P.; Pidcock, E.; Platings, M.; Shields, G. P.; Stevens, J. S.; Towler, M.; Wood, P. A. Mercury 4.0: from visualization to analysis, design and prediction. *J. Appl. Crystallogr.* **2020**, *53* (1), 226−235.
(48) Spek, A. L. Single-crystal structure validation with the program PLATON. *J. Appl. Crystallogr.* **2003**, *36* (1), 7−13.
(49) Ward, M. D. Design of crystalline molecular networks with charge-assisted hydrogen bonds. *Chem. Commun.* **2005**, No. 47, 5838−42.
(50) Hasa, D.; Miniussi, E.; Jones, W. Mechanochemical Synthesis of Multicomponent Crystals: One Liquid for One Polymorph? A Myth to Dispel. *Cryst. Growth Des.* **2016**, *16* (8), 4582−4588.
(51) Belenguer, A. M.; Lampronti, G. I.; Cruz-Cabeza, A. J.; Hunter, C. A.; Sanders, J. K. M. Solvation and surface effects on polymorph stabilities at the nanoscale. *Chem. Sci.* **2016**, *7* (11), 6617−6627.
(52) Lombard, J.; le Roex, T.; Haynes, D. A. Competition between Hydrogen and Halogen Bonds: The Effect of Solvent Volume. *Cryst. Growth Des.* **2020**, *20* (11), 7384−7391.
(53) d'Agostino, S.; Braga, D.; Grepioni, F.; Taddei, P. Intriguing Case of Pseudo-Isomorphism between Chiral and Racemic Crystals of rac- and (S)/(R)2-(1,8-Naphthalimido)-2-quinuclidin-3-yl, and Their Reactivity Toward I2 and IBr. *Cryst. Growth Des.* **2014**, *14* (2), 821−829.
(54) Rekis, T.; d'Agostino, S.; Braga, D.; Grepioni, F. Designing Solid Solutions of Enantiomers: Lack of Enantioselectivity of Chiral Naphthalimide Derivatives in the Solid State. *Cryst. Growth Des.* **2017**, *17* (12), 6477−6485.
(55) Burger, A.; Ramberger, R. J. M. A. On the polymorphism of pharmaceuticals and other molecular crystals. II. *Microchim. Acta* **1979**, *72* (3−4), 273−316.
(56) Dalhus, B.; Gorbitz, C. H. Structural relationships in crystals accommodating different stereoisomers of 2-amino-3-methylpentanoic acid. *Acta Crystallogr., Sect. B: Struct. Sci.* **2000**, *56* (4), 720−727.

https://doi.org/10.1021/acs.cgd.1c00216
Cryst. Growth Des. 2021, 21, 3438−3448